Synchronization of chemical noise-sustained structures in asymmetrically coupled differential-flow reactors

Gonzalo G. Izús* and Alejandro D. Sánchez†

IFIMAR (Universidad Nacional de Mar del Plata and CONICET), Deán Funes 3350, B7602AYL Mar del Plata, Argentina

(Received 31 December 2012; revised manuscript received 13 September 2013; published 5 December 2013)

The differential-flow-induced chemical instability is investigated in the context of two coupled reactors with cubic autocatalytic kinetics (the Gray-Scott model). Previous results for master-slave arrangement [Izús, Deza, and Sánchez, J. Chem. Phys. **132**, 234112 (2010)] are extended in this study to include bidirectional coupling between reactions. Numerical simulations in the convectively unstable regime show that synchronized noise-sustained structures are developed in both reactors due to the selective amplification of noise. A theoretical analysis shows that the nature of the synchronization and the stability of the synchronized manifold are related with the properties of the critical modes.

DOI: 10.1103/PhysRevE.88.062909 PACS number(s): 05.45.Xt, 05.40.Ca, 82.40.Bj

I. INTRODUCTION

The differential-flow-induced chemical instability (DIFICI) [1,2] is a well-established mechanism for pattern formation that presents inherent differences with the more widely investigated Turing instability. In the latter, steady waves or patterns in the reactant concentrations are formed through a diffusion-driven mechanism according to which fluctuations in reactant concentrations self-organize spontaneously out of a nonstructured medium as a consequence of the competition between autocatalytic reaction steps and differential diffusivities of activator and inhibitor species. However, key species can be disengaged by their differential transport and homogeneous steady states may be destabilized by flows of activator and inhibitor at different flow rates in the DIFICI mechanism. This instability was predicted [1] and experimentally observed [2] by Menzinger and Rovinsky for the ferroin catalyzed Belousov-Zhabotinsky reaction in a quasi-one-dimensional flow tube.

Experimental observation of DIFICI requires a differential-flow reactor, a device where some of the reactants are immobilized within the reactor while the rest of the reactive species are allowed to diffuse and flow freely. For instance, in the so-called packed-bed reactors a solid matrix (usually a cation exchange resin) is packed inside the reactor in such a way that it immobilizes one reactant, while the remaining reactive species flow and diffuse [2]. In cross-flow reactors one may resort to semipermeable membranes or discrete injection and removal ports positioned along the reactor axis, allowing one to keep the system uniformly far from equilibrium [3].

The convective nature of the DIFICI mechanism was recognized in numerical simulations [4] and theoretically established for the Brusselator [5] and the Gray-Scott (GS) kinetics [6,7]. Some extensions include cases where all the reactants flow at different rates through the reactor [8]. In the convectively unstable regime, local perturbations of the steady state are advected more rapidly than their rate of spreading and the system is driven out of its steady state toward a new state where, by dynamical amplification of noise, a macroscopic pattern called a noise-sustained structure (NSS) is continuously formed and regenerated [9]. This is the main difference with the absolutely unstable regime where perturbations grow everywhere in time and eventually contaminate the entire system. In fluid convection experiments, for instance, the NSS observed in both Taylor-Couette [10,11] and open flow [12] configurations are a macroscopic manifestation of amplified thermal fluctuations. Another possibility for self-organization in convectively unstable systems requires a permanent perturbation at the boundary. Examples thereof are a time-oscillating source [13] or a constant displacement away from the homogeneous steady state of the system [14].

As stated before, a model system where the convective nature of the DIFICI mechanism has been theoretically established is the Gray-Scott model [15], a variant of the autocatalytic Selkov model of glycolysis [16], based on the reaction between a substrate A and the autocatalyst B in a three-step kinetic scheme, the intermediate step having cubic autocatalytic kinetics:

$$P \xrightarrow{k_0} A$$
$$A + 2B \xrightarrow{k_1} 3B$$
$$B \xrightarrow{k_2} C.$$

Here the k_i $(i = 0,1,2)$ are constants and the system is kept out of equilibrium by feeding the precursor P and removing the product C.

Numerical simulations of the GS system have revealed a set of strikingly complex patterns [17], including self-replicating ones: pulses in one dimension [18–22] and spots in two dimensions [17,23]. Reaction-diffusion GS models are now frequently used to generate spatiotemporal chaos [24,25], whose control and eventual synchronization is an active research topic for its promising applications [26]. For example, spatiotemporal chaos synchronization in pairs of unidirectionally coupled reaction-diffusion GS equations has been analyzed in Ref. [27]. In the same sense, the effect of noise on the GS dynamics has been considered in the context of intermittence [28], control and characterization of spatiotemporal chaos [29,30], or effects induced by internal reaction noise [31], to cite a few examples where noise plays a relevant role. Having a rich variety of spatiotemporal patterns, the GS system is a suitable computational model to explore new pattern formation phenomena in reaction-diffusion systems.

*izus@mdp.edu.ar
†sanchez@mdp.edu.ar

In the following, we assume the GS reaction to take place in a one-dimensional (1D) differential-flow reactor where species A is immobilized along the bed reactor by an exchange resin, whereas B is advected by the flow and is also free to diffuse. This is a well-established technology to obtain differential diffusivities in the context of chemical reactions [2,32]. Note that a particular reactor geometry is required because on one hand, it is the precursor P what is injected at constant rate and on the other, its immediate product A must be immobilized.[1]

After scaling concentrations by $(k_2/k_1)^{1/2}$, time by k_2^{-1}, and length by $(D_B/k_2)^{1/2}$, the GS rate equations read

$$\frac{\partial a}{\partial t} = \mu - a\,b^2 + \xi(x,t), \tag{1}$$

$$\frac{\partial b}{\partial t} = \frac{\partial^2 b}{\partial x^2} - \phi\,\frac{\partial b}{\partial x} - b + a\,b^2, \tag{2}$$

where μ stands for the scaled version of $k_0 p_0$ and ϕ for that of the fluid velocity v. The real Gaussian noise ξ, with zero mean and $\langle \xi(x,t)\xi(x',t')\rangle = 2\eta\delta(x-x')\delta(t-t')$, in the rate equation for a accounts for fluctuations in p_0. For $\mu > 1$, the uniform steady state $b = a^{-1} = \mu$ becomes convectively unstable at a finite wavelength for a critical value $\phi_c(\mu)$ [6]. A complete derivation, including the validation of the polled-chemical approximation inherent in Eqs. (1) and (2) is given in Refs. [33,34].

Noise-sustained structures have been predicted and numerically observed for Eqs. (1) and (2) above threshold ϕ_c (see Ref. [35] for further details). In particular, NSS in the GS model can be replicated through appropriate coupling between reactors. In Refs. [36,37] we have shown that unidirectional coupling in the autocatalytic component originates synchronized NSS, for both uniform (1D) and Poiseuille (2D) flows. A feature of the master-slave coupling is its ability to replicate the NSS in the coupled reactor with a high degree of correlation. Note that this is an example of synchronization between extended systems, which is formulated in terms of the dynamics of unidirectionally coupled nonlinear fields. In fact, arrays of coupled oscillators appear ubiquitously in nature, and their mutual synchronization is one of the highly intriguing phenomena arising in complex systems [38]. In particular, the synchronization of coupled chaotic systems has been an intensively studied topic since 1990 [39], its effects having been explored in natural phenomena and laboratory experiments [40–43]. An active field of research for its potential applications is the study of synchronization phenomena in spatially extended systems, such as populations of coupled chaotic units and neural networks [44–48], coupled map lattices [49], and continuous systems ruled by partial differential equations [27,50–52]. Among them, the synchronization of extended chemical reactions has become a relevant field for its experimental observations, as, e.g., the synchronization of Belousov-Zhabotinsky reactions in extended flowing systems [53], locally coupled reactions [54,55], or interacting microreactors [56]. In most cases, synchronization studies have mainly considered bidirectional symmetric or unidirectional master-slave coupling configurations. In many practical situations, however, it is not expected to have purely unidirectional nor perfectly symmetric coupling [57]; quantifying asymmetries in the coupling scheme is relevant in applications such as the study of the human cardiorespiratory system [58]. For instance, Ref. [59] has shown that asymmetry in the coupling of two 1D complex Ginzburg-Landau equations enhances the synchronization and plays an important role in controlling the synchronized dynamics. The characterization of the synchronization between NSS under general couplings results, in consequence, are of interest to elucidate the robustness of the phenomena and to clarify the role of the coupling structure in the process of NSS replication.

Our aim is to investigate the synchronization between NSS generated by the DIFICI mechanism in *bidirectionally* coupled reactors with cubic kinetics and additive noise, by considering the possibility of asymmetric coupling. Synchronized NSS are numerically observed and theoretically analyzed. The theoretical stability-analysis results for both the uniform steady state and the synchronized manifold are checked against numerical simulations, which confirm the predicted thresholds and their dependence on the couplings.

The paper is organized as follows. Section II presents the equations of the coupled reactors, the linear stability analysis of the uniform solution, and the features of the critical modes. Section III illustrates the synchronization of NSS under bidirectional coupling, characterizing the typical features of the structures and their correlations. Section IV sketches the stability of the synchronized manifolds in terms of a damped dynamics of Fourier modes. Finally, the main conclusions are summarized in Sec. V.

II. SYSTEM

In this work, we consider two identical reactors coupled in a not necessarily symmetric way:

$$\frac{\partial a_1}{\partial t} = \mu - a_1\,b_1^2 + \xi_1(x,t), \tag{3}$$

$$\frac{\partial b_1}{\partial t} = \frac{\partial^2 b_1}{\partial x^2} - \phi\,\frac{\partial b_1}{\partial x} - b_1 + a_1\,b_1^2 + \epsilon_{12}(b_2 - b_1), \tag{4}$$

$$\frac{\partial a_2}{\partial t} = \mu - a_2\,b_2^2 + \xi_2(x,t), \tag{5}$$

$$\frac{\partial b_2}{\partial t} = \frac{\partial^2 b_2}{\partial x^2} - \phi\,\frac{\partial b_2}{\partial x} - b_2 + a_2\,b_2^2 + \epsilon_{21}(b_1 - b_2). \tag{6}$$

ξ_1 and ξ_2 are uncorrelated white noises with the same intensity η, and ϵ_{12} and ϵ_{21} denote the corresponding coupling strengths. While positive values of the latter correspond to diffusive coupling, negative coupling strengths correspond to "active" interaction where reactants must "climb" gradients of concentration. Although there are examples of this behavior in the context of biological systems, such as sodium and potassium pumps in cell membranes [60], the implementation of active couplings in the context of extended chemical reactions is not straightforward, requiring a continuous passive measure of reactive species along the reactor and pumps that create the corresponding cross flows by injecting reactants and

[1]For example the resin can be a previously loaded plate, which is continuously fed from one surface while the reaction takes place in the opposite one, where A remains fixed. Particular reactor aspect ratios must be also considered in order to have an effective quasi-one-dimensional reaction.

removing products.[2] Nevertheless, full characterization of the sync dynamics demands including this case. In fact some of the results shown below can be applied in the more general framework of coupled nonlinear oscillators. In the context of neural arrays, e.g., the active coupling corresponds to the antiphase one, experimentally observed in human epileptic astrocyte cultures [62] and numerically investigated in neural arrays [62,63].

Equations (3)–(6) have a stationary uniform solution, given by $b_1 = b_2 = a_1^{-1} = a_2^{-1} = \mu$. Its linear stability can be obtained in the usual way, through a small perturbation to the solution of the form

$$a_1 = 1/\mu + \Delta a_1 \exp(ikx + \sigma t), \tag{7}$$

$$b_1 = \mu + \Delta b_1 \exp(ikx + \sigma t), \tag{8}$$

$$a_2 = 1/\mu + \Delta a_2 \exp(ikx + \sigma t), \tag{9}$$

$$b_2 = \mu + \Delta b_2 \exp(ikx + \sigma t). \tag{10}$$

Inserting these expressions in (3)–(6) and keeping only linear terms in departures from the stationary state, the following eigenvalue problem results:

$$\sigma \Delta a_1 = -\mu^2 \Delta a_1 - 2\Delta b_1 \tag{11}$$

$$\sigma \Delta b_1 = \mu^2 \Delta a_1 + (1 - \epsilon_{12} - k^2 - i\phi k)\Delta b_1 + \epsilon_{12}\Delta b_2 \tag{12}$$

$$\sigma \Delta a_2 = -\mu^2 \Delta a_2 - 2\Delta b_2 \tag{13}$$

$$\sigma \Delta b_2 = \epsilon_{21}\Delta b_1 + \mu^2 \Delta a_2 + (1 - \epsilon_{21} - k^2 - i\phi k)\Delta b_2, \tag{14}$$

which can be exactly solved. Introducing the functions

$$S(z) = 1 - z - i\phi k - k^2 - \mu^2, \tag{15}$$

$$R(z) = \sqrt{S(z)^2 - 4(1 + z + i\phi k + k^2)\mu^2}, \tag{16}$$

the four eigenvalues read

$$\sigma_{1,2} = \tfrac{1}{2}[S(0) \mp R(0)], \tag{17}$$

$$\sigma_{3,4} = \tfrac{1}{2}[S(2\epsilon) \mp R(2\epsilon)], \tag{18}$$

where $\epsilon = (\epsilon_{12} + \epsilon_{21})/2$ denotes the mean coupling. Note that $\sigma_{1,2}$ depend on ϕ, k, and μ, while $\sigma_{3,4}$ depend also on ϵ. The eigenvectors are given by

$$(\Delta a_1, \Delta b_1, \Delta a_2, \Delta b_2)_{1,2} = \left(\frac{4}{-S(0) \pm R(0) - 2\mu^2}, 1, \frac{4}{-S(0) \pm R(0) - 2\mu^2}, 1\right) \tag{19}$$

$$(\Delta a_1, \Delta b_1, \Delta a_2, \Delta b_2)_{3,4} = \left(\frac{4\,\epsilon_{12}/\epsilon_{21}}{S(2\epsilon) \mp R(2\epsilon) + 2\mu^2}, -\frac{\epsilon_{12}}{\epsilon_{21}}, \frac{-4}{S(2\epsilon) \mp R(2\epsilon) + 2\mu^2}, 1\right). \tag{20}$$

[2]Another possibility (in the context of photosensitive chemical reactions) is to introduce the coupling through a mask of illumination, whose intensity is related to the (optically measured) difference of concentrations, as reported in Ref. [61] for the synchronization of two extended Belousov-Zhabotinsky reactions.

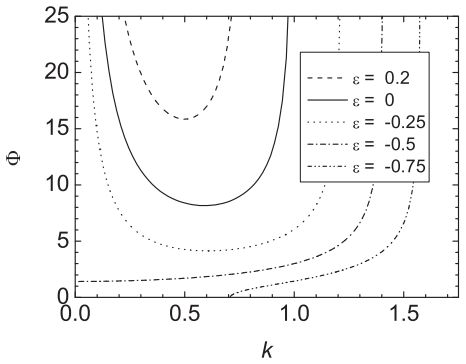

FIG. 1. Plot of the Φ function for $\mu = 2$ and different values of ϵ. The $\epsilon = 0$ instability takes place at $k_c = 0.592$ for $\phi_c = 8.16$. For $\epsilon < -0.5$ the system is unstable still in the absence of flow.

While the eigenvectors corresponding to $\sigma_{1,2}$ have the same parameter dependence as their eigenvalues, the ones corresponding to $\sigma_{3,4}$ also include a dependence on the ratio $\epsilon_{12}/\epsilon_{21}$. The form of the eigenvectors is also of relevance for our analysis: the ones corresponding to the "1–2" branch are in phase ($\Delta a_1 = \Delta a_2$, $\Delta b_1 = \Delta b_2$) whereas the relative amplitude and sign can change in the second one ($\Delta a_1/\Delta a_2 = \Delta b_1/\Delta b_2 = -\epsilon_{12}/\epsilon_{21}$).

As soon as $\mathrm{Re}(\sigma_j) > 0$ for any j, the solution becomes unstable. Just at the instability point, σ_j is an imaginary number. Replacing $\sigma_j = i\lambda$ (with real λ) into Eqs. (11)–(14), we obtain the characteristic equation, which in this situation factorizes into two complex equations. Each one of them gives a relation between the flux velocity and the wave number k. Defining the function

$$\Phi(z,k) = \frac{\mu^2 + k^2 + z - 1}{|k|}\sqrt{\frac{1 + k^2 + z}{1 - k^2 - z}} \tag{21}$$

we have

$$\phi_1 = \Phi(0,k), \tag{22}$$

$$\phi_2 = \Phi(2\epsilon,k), \tag{23}$$

where ϕ_1 (ϕ_2) correspond to the instability of $\sigma_{1,2}$ ($\sigma_{3,4}$). In Fig. 1 we show both branches of Φ as functions of k (ϕ_1 in solid line). The minimum of ϕ_1 corresponds to the

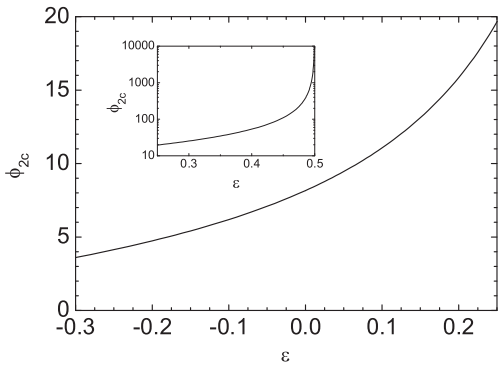

FIG. 2. ϕ_{2c} as function of ϵ for $\mu = 2$. The inset shows a wider range of values in a logarithmic scale.

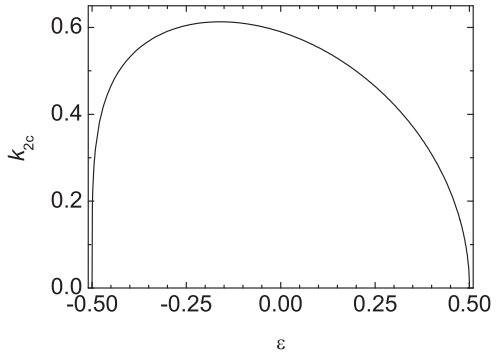

FIG. 3. k_{2c} as function of ϵ for $\mu = 2$.

critical value ϕ_c, which is independent on the couplings. For $\phi > \phi_c$ and positive mean coupling it is the first mode that destabilizes. In contrast, the second branch ϕ_2 is associated to larger or lower values of ϕ, depending on whether $\epsilon > 0$ or $\epsilon < 0$, respectively. For both cases, its minimum value (ϕ_{2c}) corresponds to the destabilization of the second branch of eigenvectors $\sigma_{3,4}$. As we will see later, both thresholds have physical meaning. Note that for $\epsilon > 0$ ($\epsilon < 0$) the critical flow velocity of the finite-wavelength instability is determined by ϕ_c (ϕ_{2c}). The critical value ϕ_{2c} and its critical wave vector k_{2c} as a function of ϵ are shown in Figs. 2 and 3, respectively. The values k_c and ϕ_c can be read off in the corresponding figure at $\epsilon = 0$.

For $\epsilon_{12} = \epsilon_{21} = 0$, Eqs. (3)–(6) describe two uncoupled reactions, identical with regard to the parameters but submitted to independent spatiotemporal noises. NSS have been reported in this case for $\phi > \phi_c$ [35]. For $\epsilon_{12} = 0$ and $\epsilon_{21} > 0$, Eqs. (3)–(6) describe two unidirectionally coupled reactions, for which replicated NSS have been reported in Ref. [37] in the convectively unstable regime. This master-slave configuration presents the same threshold of convective instability as a single reactor. We conclude that this is a general property associated to arbitrary couplings satisfying $\epsilon > 0$.

To discriminate between convective and absolute instabilities we need to analyze the eigenvalues in the complex k plane. The asymptotic linear behavior of arbitrary wave packets can be obtained using the method of steepest descent [64]. Following Refs. [6,9], we determine the saddle point [root of $\partial_k \sigma(k) = 0$] as $k_s = -i\phi/2$. Evaluating the eigenvalues (17) and (18) at k_s, we find that the uniform state is stable ($\phi < \phi_c$ or $\phi < \phi_{2c}$ for ϵ positive o negative, respectively) or convectively

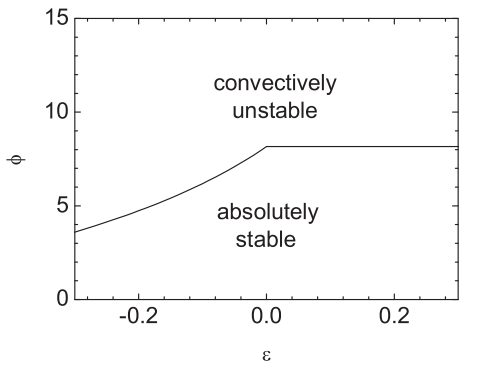

FIG. 4. The different stability regimes for $\mu = 2$.

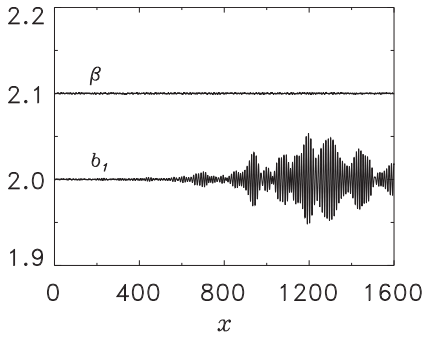

FIG. 5. Pattern b_1 and β (shifted) as a function of the space variable x for $\phi = 8.8$ ($\phi_c = 8.16$), $\epsilon_{12} = \epsilon_{21} = 0.04$ and $t = 1.2 \times 10^6 \Delta t$. A similar picture (not shown) is obtained for a_1 and α.

unstable ($\phi > \phi_c$ or ϕ_{2c}) if μ and ϵ satisfy $\epsilon > -1/2$ and $\mu > \sqrt{1-2\epsilon}$, respectively. A diagram of the situation is shown in Fig. 4 for $\mu = 2$. In addition, a regime of absolute instability is found for $\epsilon < -1/2$ and $\phi < \phi_a(\epsilon) = 2\sqrt{-2\epsilon - 1}$, while the instability becomes convective for $\phi > \phi_a(\epsilon)$ (that zone is not in the ϵ range displayed in Fig. 4, see footnote in Sec. III).

III. NUMERICAL RESULTS

Equations (3)–(6) have been integrated using an Euler stochastic scheme in a grid of $N = 16384$ sample points with a space step $\Delta x = 0.1$ and time step $\Delta t = 10^{-4}$. Throughout the paper $\eta = 10^{-7}$, $\mu = 2$, and the length $L = N\Delta x$ are chosen in such a way that spatiotemporal patterns develop well before they reach the outlet. For each system, Dirichlet BC are assumed at the inlet of the reaction domain $[a_1(0,t)^{-1} = a_2(0,t)^{-1} = b_1(0,t) = b_2(0,t) = \mu]$ and Neumann BC at the outlet $x = L$.

Equations (22) and (23) indicate that the coupling dependence of the critical values is only through ϵ. We first analyze the case $\epsilon > 0$. The linear stability analysis predicts that NSS are expected in both reactors for $\phi > \phi_c$. Numerical simulations confirm this fact and synchronized NSS are observed in this regime. We illustrate this point in Fig. 5, where

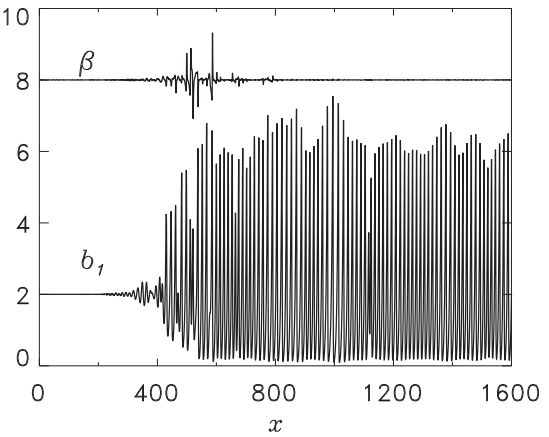

FIG. 6. Similar magnitudes as in Fig. 5, for higher flow velocity. The parameters are $\phi = 22$, $\epsilon_{12} = 0.1125$, $\epsilon_{21} = 0.0675$, and $t = 6 \times 10^5 \Delta t$.

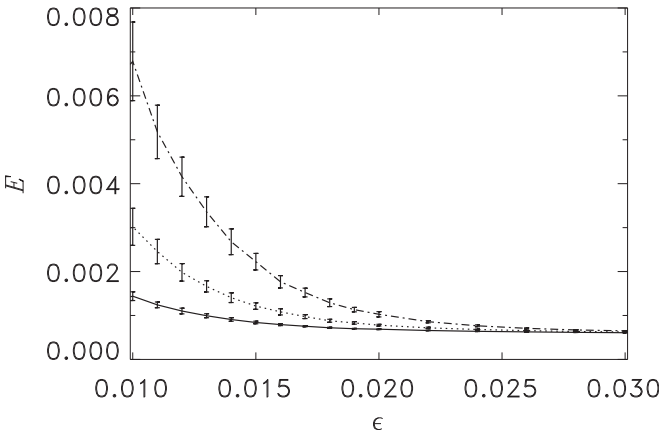

FIG. 7. E vs ϵ, averaged over 40 realizations for ϕ near threshold. Here $\epsilon = \epsilon_{12} = \epsilon_{21}$. Solid, dotted and dashed-dotted lines correspond to $\phi = 8.6$, $\phi = 8.7$, and $\phi = 8.8$, respectively. Here $t = 2.4 \times 10^6 \Delta t$.

we show a snapshot of the emerging patterns near threshold and also the deviation fields

$$\alpha(x,t) = a_1(x,t) - a_2(x,t),$$
$$\beta(x,t) = b_1(x,t) - b_2(x,t). \tag{24}$$

Near the critical point, the structures have small amplitude. For larger values of ϕ, well-developed synchronized NSS are observed in both reactors, as shown in Fig. 6.

In order to quantify the synchrony, the global synchronization error

$$E(t) = \sqrt{\frac{1}{L}\int_0^L [\alpha^2(x,t) + \beta^2(x,t)]\,dx}, \tag{25}$$

is introduced. We numerically observe that the degree of correlation depends on the mean coupling strength ϵ, as predicted. This fact has been numerically checked for a wide range of situations. In Fig. 7 we plot E vs ϵ for flow velocities

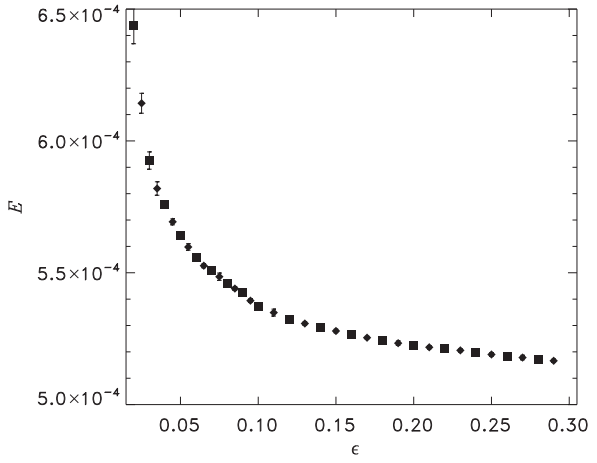

FIG. 8. E vs ϵ, averaged over 20 realizations. Diamonds correspond to $\epsilon_{12} = 1.25\,\epsilon$ and $\epsilon_{21} = 0.75\,\epsilon$, while squares correspond to $\epsilon_{12} = 1.65\,\epsilon$ and $\epsilon_{21} = 0.35\,\epsilon$. The remaining parameters are $\phi = 8.8$ and $t = 1.4 \times 10^5$.

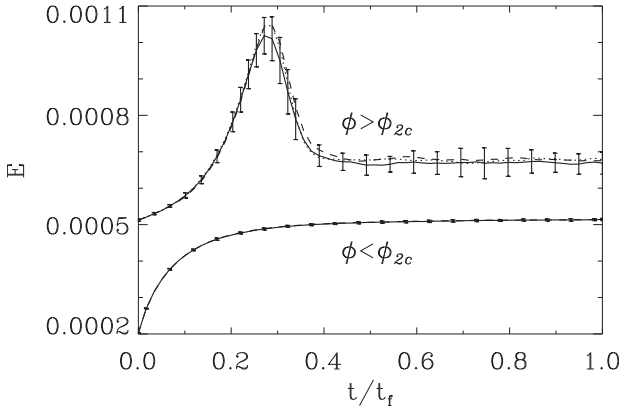

FIG. 9. Global synchronization error E vs t averaged over 40 realizations. The coupling values are: $\epsilon_{12} = 0.1, \epsilon_{21} = 0.3$ (solid line); $\epsilon_{12} = 0.15$, $\epsilon_{21} = 0.25$ (dotted line); $\epsilon_{12} = 0.2$, $\epsilon_{21} = 0.2$ (dashed line), while the remaining parameters are $\phi = 21$ (upper curves), $\phi = 16$ (lower curves). For clarity, only error bars corresponding to the solid line are showed. All coupling combinations correspond to $\epsilon = 0.2$. The time scales are $t_f = 7.5 \times 10^5 \Delta t$ (upper curves) and $t_f = 12480 \Delta t$ (lower curves).

near the critical value. We stress the robustness of the obtained results, which keep their degree of correlation determined by ϵ, as illustrated in Fig. 8 for larger values of the mean coupling.

Watching the temporal evolution of E, one sees a different qualitative behavior whether $\phi < \phi_{2c}$ or $\phi > \phi_{2c}$. While below ϕ_{2c} the error grows monotonically and saturates, for $\phi > \phi_{2c}$ the same synchronization phenomenon is observed asymptotically, but now the error grows for short times indicating a lack of synchrony in the linear regime (related to the destabilization of the second branch of eigenvalues). When the structures are well developed, the systems eventually synchronize and the error relaxes to its asymptotic value, as illustrated in Fig. 9. Note the different time scale of each curve in the figure.

Now we consider the case $\epsilon < 0$. We limit the analysis of active couplings to the region $-0.3 \lesssim \epsilon$, where the

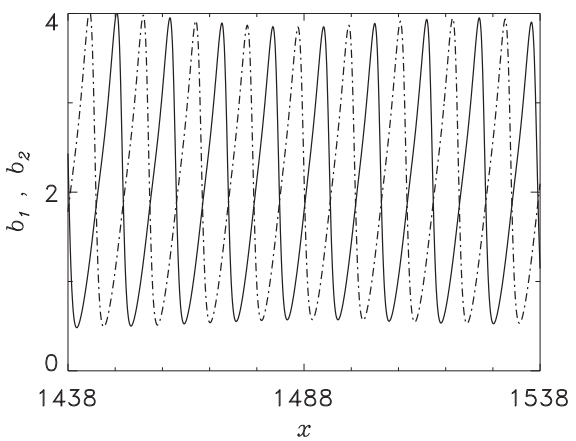

FIG. 10. Detail of patterns in the B species for both reactors with symmetric negative coupling. The parameters are $\epsilon_{12} = \epsilon_{21} = -0.1$, $\phi = 7.5$ and $t = 2.5 \times 10^5 \Delta t$. In solid (dashed) line b_1 (b_2).

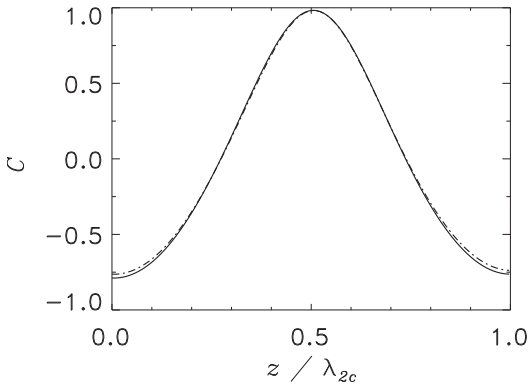

FIG. 11. Correlation for patterns in Fig. 10: $C_{b_1b_2}$ (solid line) and $C_{a_1a_2}$ (dashed dotted line). The spatial variable was scaled with $\lambda_{2c} = 2\pi/k_{2c}$.

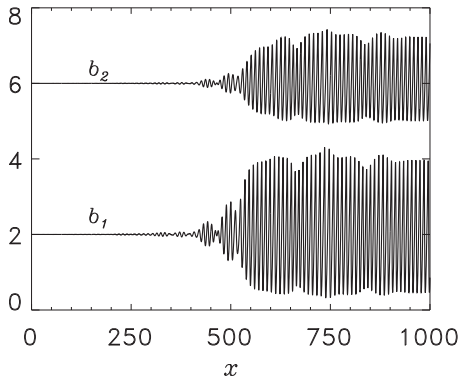

FIG. 12. Snapshot of the patterns in the B species for both reactors (b_2 shifted). The parameters used in the simulations are $\epsilon_{12} = -0.05$, $\epsilon_{21} = -0.15$, $\phi = 7.5$, and $t = 2.5 \times 10^5 \Delta t$. Note that ϵ and the rest of parameters, except individual coupling, are the same as those of Fig. 10.

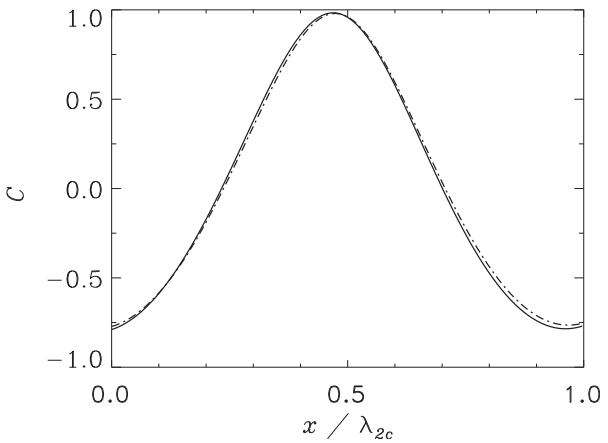

FIG. 13. Correlation for patterns in Fig. 12: $C_{b_1b_2}$ (solid line) and $C_{a_1a_2}$ (dashed dotted line).

concentrations of all species remain positive.[3] The linear stability analysis also leads to expect NSS in both reactors for $\phi > \phi_{2c}$. Numerical simulations confirm this prediction and synchronized NSS are also observed in this regime. For $\epsilon_{12} = \epsilon_{21}$ the resulting structures have the same amplitudes, but they are shifted in half a wavelength, as observed in Fig. 10. To quantify the phenomenon, we introduce the cross-correlation function

$$C_{pq}(t,z) = C\{p(x,t),q(x,t),z\} = \int [p(x+z,t) - \langle p(x,t)\rangle] \times [q(x,t) - \langle q(x,t)\rangle]\, dx/\sqrt{\sigma(p)\sigma(q)}, \quad (26)$$

where p and q can be $a_{1,2}$ or $b_{1,2}$, $\langle . \rangle$ denotes mean value in space and $\sigma(.)$ denotes variance. In Fig. 11 we plot $C_{b_1b_2}$ and $C_{a_1a_2}$ as a function of z, for the well-developed NSS illustrated in Fig. 10: a maximum of order one is observed at $z = \pi/k_{2c}$.

For $\epsilon_{12} \neq \epsilon_{21}$, a similar behavior for the correlation is observed (although the structures have different amplitudes, as illustrated in Fig. 12). Again the maximum correlation is observed at $z = \pi/k_{2c}$, as shown in Fig. 13.

IV. STABILITY OF THE SYNCHRONIZATION MANIFOLD

As in Ref. [35] the critical modes determine the kind of NSS to be observed above threshold. For $\epsilon > 0$ the threshold is independent of the couplings, while for $\epsilon < 0$ this situation changes and NSS are numerically observed for lower values of ϕ.

Since reactors 1 and 2 synchronize in both cases, manifolds $a_1 = a_2$ and $b_1 = b_2$ are expected to be at least linearly stable. In particular, the linear stability analysis for (α,β) around the uniform rest state goes through as in Ref. [36], and the same occurs for the stability around the stochastic macroscopic structures. A similar synchronization scenario, related with a damped dynamics of the deviation field's Fourier modes, remains valid. The stability analysis around the uniform solution confirms that the synchronization manifold is linearly stable for $\phi > \phi_c$ ($\epsilon > 0$) or $\phi > \phi_{2c}$ ($\epsilon < 0$). For positive (negative) ϵ they become convectively unstable above ϕ_{2c} (ϕ_c).[4]

V. CONCLUSIONS

We have investigated the formation and synchronization of noise-sustained structures in one-dimensional differential-flow reactors with cubic kinetics (Gray-Scott model) and linear couplings in the inhibitor components. By coupling the corresponding points of both reactors bidirectionally, we

[3]We numerically observe the possibility to obtain negative concentrations for smaller coupling values. For chemically active coupling, the ϵ_{ij} should be $\epsilon_{ij}\theta(b_j)$ in order that the concentration be non-negative (being θ the step function). Nevertheless this correction does not change the stability analysis and further considerations.

[4]The equations for the stability of the synchronized manifold in Ref. [36] remain valid by changing the master-slave coupling ϵ by $2\epsilon = \epsilon_{12} + \epsilon_{21}$ in the general case.

have shown that appropriate values of the external flow rates drive the dynamics toward a convectively unstable regime, where complete synchronization of the emerging macroscopic noise-sustained structures is achieved. The usual estimators of synchrony, such as correlations or global sync error, indicate that twin structures can be obtained for appropriate value of strength couplings and flow velocity. We have also shown that the correlation is present point-to-point and this means that the phenomenon is spatially distributed.

From the theoretical point of view we have performed the linear instability analysis of the steady-state solution. That analysis reveals the existence of two branches of eigenvalues, one of them independent of couplings, while the other one depends on the average coupling value ϵ. We remark that this is a generic property of the considered couplings. In fact, it can be proved that Eqs. (3)–(6), with arbitrary nonlinearities but the same linear coupling, diffusion, and flow terms, originate a similar behavior of the eigenvalues: a branch independent of the couplings and the other one depending on couplings only through ϵ. As usual, instabilities are associated with the lower branch and the parameters must be specified in order to identify the critical mode. Equations (22) and (23) are a good example of that: while the ϵ-independent branch is the critical one for positive ϵ, the ϵ-dependent branch is the critical one for negative ϵ. In both cases, the instability takes place at finite wavelength, providing the route to pattern formation.

An important point when addressing issues related to experimental observation of synchronization is robustness: in this respect, the dependence of sync with the structure and strength of the couplings results relevant. An important prediction of our analysis is that uncoupled, unidirectionally coupled in master-slave configuration, and bidirectionally (symmetrically or asymmetrically) coupled reactors have the *same threshold* of convective instability for $\epsilon \geqslant 0$. Numerical simulations have confirmed this result and have also shown that the emerging structures in both reactors are synchronized. We remark that our analysis imposes a restricted scenario to reaction-diffusion-advection systems with DIFICI mechanisms, and linearly coupled in the diffusive species. Key indicators (such as critical flow velocity or wavelength) can depend on coupling only through ϵ, and this fact opens interesting possibilities. For instance, several properties of bidirectionally coupled reactions could be first characterized in terms of the master-slave ones, without loss of generality. The linear stability analysis of the synchronized manifold around the uniform solution confirms this fact and also predicts a convective instability when the ϵ-dependent branch becomes critical. This instability has been numerically verified and we have shown that in this regime the systems exhibit an initial lack of synchrony. In all the cases, the reactors eventually synchronize and the stability analysis presented in Ref. [36] for unidirectional couplings can be applied in this case. An effective dynamics (in terms of damped Fourier modes for the stability of the synchronized manifolds) eventually drives the dynamics to the sync regime.

The eigenvalue branches exchange their relative stabilities for negative ϵ, and the ϵ-dependent branch becomes critical at a finite wavelength for some value of the external flow velocity. In this regime we have shown that the system can self-organize with smaller values of flow velocity and synchronized structures appear, but now with a shift of half a wavelength in space if both couplings have the same sign. This particularity can be traced back to the structure of the critical mode of the second branch, where the possibility to have a relative negative sign in the components originates the spatial shift. Even more, the observed relative amplitude between the noise-sustained structures is in qualitative agreement with the eigenvector structure. For symmetric couplings both patterns have the same amplitude, while structures with different amplitudes are developed in each reactor in the asymmetric case. As a limit case, unidirectional coupling in this regime can originate a noise-sustained structure in the coupled reactor while the other one remains in the steady state, reflecting the fact that the modes of the uncoupled reactor remain damped in this regime. Note that this scenario is different from the one reported in Ref. [36], where the master-slave configuration starts from the destabilization of the master reactor and the emerging structure is finally replicated in the slave one.

We finally point out that the imposed flow breaks in a generic way the spatial symmetry of the coupled systems for any reaction, allowing eventual convective instabilities. In the same sense, the imposed coupling factorizes the eigenvalue spectrum for reaction-diffusion-advection systems in a characteristic way, where the dependence of thresholds on the coupling strengths results particularly restricted. Thus, we expect synchronized chemical noise-sustained structures to be observed in coupled flow-reactors under general conditions. In this sense, we hope our study will qualitatively apply to other reactions with DIFICI mechanism.

ACKNOWLEDGMENTS

This work was supported by Universidad Nacional de Mar del Plata, Argentina, by Grant No. EXA 603/12 and CONICET through project PIP 12220100100315. We tank R. Deza for a critical reading of the manuscript.

[1] A. B. Rovinsky and M. Menzinger, Phys. Rev. Lett. **69**, 1193 (1992).
[2] A. B. Rovinsky and M. Menzinger, Phys. Rev. Lett. **70**, 778 (1993).
[3] V. Z. Yakhnin, A. B. Rovinsky, and M. Menzinger, Chem. Eng. Sci. **50**, 2853 (1995).
[4] X. G. Wu, S. Nakata, M. Menzinger, and A. Rovinsky, J. Phys. Chem. **100**, 15810 (1996).
[5] M. Sangalli and H. C. Chang, Phys. Rev. E **49**, 5207 (1994).
[6] R. A. Satnoianu, J. H. Merkin, and S. K. Scott, Physica D **124**, 345 (1998).
[7] R. A. Satnoianu, J. H. Merkin, and S. K. Scott, Chem. Eng. Sci. **55**, 461 (2000).
[8] R. A. Satnoianu, J. H. Merkin, and S. K. Scott, Dynam. Stabil. Syst. **15**, 209 (2000).

[9] R. Deissler, J. Stat. Phys. **40**, 371 (1985); **54**, 1459 (1989); Physica D **56**, 303 (1992).

[10] K. L. Babcock, G. Ahlers, and D. S. Cannell, Phys. Rev. Lett. **67**, 3388 (1991).

[11] A. Tsameret and V. Steinberg, Phys. Rev. Lett. **67**, 3392 (1991).

[12] M. A. Scherer and G. Ahlers, Phys. Rev. E **65**, 051101 (2002).

[13] P. Huerre, in *Instabilities and Nonequilibrium Structures*, edited by E. Tirapegui and D. Villlaroel (Reidel, Dordrecht, 1987), pp. 141–177.

[14] S. P. Kuznetsov, E. Mosekilde, G. Dewel, and P. Borckmanns, J. Chem. Phys. **106**, 7609 (1997).

[15] P. Gray and S. K. Scott, Chem. Eng. Sci. **38**, 29 (1983); **39**, 1087 (1984); J. Phys. Chem. **89**, 22 (1985).

[16] E. E. Selkov, Eur. J. Biochem. **4**, 79 (1968).

[17] J. E. Pearson, Science **261**, 189 (1993).

[18] W. N. Reynolds, J. E. Pearson, and S. Ponce-Dawson, Phys. Rev. Lett. **72**, 2797 (1994).

[19] N. Parekh, V. R. Kumar, and B. D. Kulkarni, Phys. Rev. E **52**, 5100 (1995).

[20] W. N. Reynolds, S. Ponce-Dawson, and J. E. Pearson, Phys. Rev. E **56**, 185 (1997).

[21] Y. Nishiura and D. Ueyama, Physica D **130**, 73 (1999).

[22] M. R. Roussel and J. Wang, Phys. Rev. Lett. **87**, 188302 (2001).

[23] C. B. Muratov and V. V. Osipov, Eur. Phys. J. B **22**, 213 (2001).

[24] A. De Wit, G. Dewel, and P. Borckmans, Phys. Rev. E **48**, R4191 (1993).

[25] R. Wackerbauer and K. Showalter, Phys. Rev. Lett. **91**, 174103 (2003).

[26] A. Khandra, X. Liu, and X. Shen, Chaos, Solitons and Fractals **26**, 615 (2005).

[27] L. Kocarev, Z. Tasev, and U. Parlitz, Phys. Rev. Lett. **79**, 51 (1997).

[28] Y. Hayase and H. R. Brand, J. Chem. Phys. **123**, 124507 (2005).

[29] C. Tao, X. Liu, and G. Du, Phys. Rev. E **81**, 046209 (2010).

[30] R. Wackerbauer and S. Kobayashi, Phys. Rev. E **75**, 066209 (2007).

[31] D. Hochberg, M. P. Zorzano, and F. Morán, J. Chem. Phys. **122**, 214701 (2005).

[32] J. Maselko and K. Showalter, Nature (London) **339**, 609 (1989).

[33] D. J. Needham and J. H. Merkin, Dynam. Stabil. Syst. **4**, 259 (1989).

[34] P. Hill, J. H. Merkin, and D. J. Needham, J. Eng. Math. **29**, 413 (1995).

[35] B. von Haeften and G. Izús, Phys. Rev. E **67**, 056207 (2003).

[36] G. G. Izús, R. R. Deza, and A. D. Sánchez, J. Chem. Phys. **132**, 234112 (2010).

[37] A. D. Sánchez, G. G. Izús, and R. R. Deza, Physica A **391**, 4070 (2012).

[38] A. Pikovsky, M. Rosenblum, and J. Kurths, *Synchronization* (Cambridge University Press, Cambridge, 2001).

[39] S. Boccaletti, J. Kurths, G. Osipov, D. L. Valladares, and C. S. Zhou, Phys. Rep. **366**, 1 (2002).

[40] K. Kaneko and I. Tsuda, *Complex Systems: Chaos and Beyond, A Constructive Approach with Applications in Life Sciences* (Springer-Verlag, Berlin, 2000).

[41] A. Winfree, *The Geometry of Biological Time* (Springer, New York, 2001).

[42] S. H. Strogatz, *Sync: The Emerging Science of Spontaneous Order* (Hyperion Press, New York, 2003).

[43] S. Manrubia, A. Mikhailov, and D. Zanette, *Emergence of Dynamical Order* (World Scientific, Singapore, 2004).

[44] S .H. Strogatz, R. E. Mirollo, and P. C. Matthews, Phys. Rev. Lett. **68**, 2730 (1992).

[45] A. Pikovsky, M. Rosenblum, and J. Kurths, Europhys. Lett. **34**, 165 (1996).

[46] J. W. Shuai and K. W. Wong, Phys. Rev. E **57**, 7002 (1998).

[47] D. H. Zanette and A. S. Mikhailov, Phys. Rev. E **58**, 872 (1998).

[48] A. Arenas *et al.*, Phys. Rep. **469**, 93 (2008).

[49] A. Pikovsky, O. Popovych, and Y. Maistrenko, Phys. Rev. Lett. **87**, 044102 (2001).

[50] H. Chaté, A. Pikovsky, and O. Rudzick, Physica D **131**, 17 (1999).

[51] L. Junge and U. Parlitz, Phys. Rev. E **62**, 438 (2000).

[52] M. A. Miranda, J. Burguete, H. Mancini, and W. Gonzalez-Viñas, Phys. Rev. E **87**, 032902 (2013).

[53] M. S. Paoletti, C. R. Nugent, and T. H. Solomon, Phys. Rev. Lett. **96**, 124101 (2006).

[54] M. Hildebrand, J. Cui, E. Mihaliuk, J. Wang, and K. Showalter, Phys. Rev. E **68**, 026205 (2003).

[55] M. Toiya, H. O. Gonzalez-Ochoa, V. K. Vanag, S. Fraden, and I. R. Epstein, J. Phys. Chem. Lett. **1**, 1241 (2010).

[56] A. F. Taylor, Z. Huang, F. Wang, M. R. Tinsley, and K. Showalter, Phys. Nonlinear Phenom. **239**, 785 (2010).

[57] M. G. Rosenblum and A. S. Pikovsky, Phys. Rev. E **64**, 045202(R) (2001).

[58] M. G. Rosenblum, L. Cimponeriu, A. Bezerianos, A. Patzak, and R. Mrowka, Phys. Rev. E **65**, 041909 (2002).

[59] J. Bragard, S. Boccaletti, and H. Mancini, Phys. Rev. Lett. **91**, 064103 (2003).

[60] X. X. Wu and J. W. Shuai, Phys. Rev. E **85**, 061911 (2012).

[61] M. Hildebrand, J. Cui, E. Mihaliuk, J. Wang, and K. Showalter, Phys. Rev. E **68**, 026205 (2003).

[62] G. Balázsi, A. Cornell-Bell, A. B. Neiman, and F. Mass, Phys. Rev. E **64**, 041912 (2001).

[63] O. Weihberger and S. Bahar, Phys. Rev. E **76**, 011910 (2007).

[64] C. M. Bender and S. A. Orszag, *Advanced Mathematical Methods for Scientists and Engineers* (McGraw-Hill, New York, 1978).